Semi-Lagrangian formulation for the advection-diffusion-absorption equation at high Péclet numbers

Albert Puigferrat[1], Miguel Masó[1], Ignasi de-Pouplana[1,2], Guillermo Casas[1,2] and Eugenio Oñate[1,2]

[1] *Centre Internacional de Mètodes Numèrics en Enginyeria CIMNE, Barcelona, Spain*
[2] *Universitat Politècnica de Catalunya (UPC), Barcelona, Spain*

Abstract

We present a numerical method for solving advective–diffusive–absorptive problems with high values of the advection. A Langrangian approach based on the updated version of the Particle Finite Element Method is used to calculate advection, while an Eulerian strategy based on the Finite Element Method (FEM) is adopted to compute its diffusion and absorption. The Eulerian FEM procedure is based on a Finite Increment Calculus (FIC) stabilized formulation recently developed by the authors. The most relevant features of each computational approach are outlined and the coupling scheme is explained. Several problems are solved to validate the method: the evolution of a localized concentration field in two dimensions (2D), the evolution of a spherical field in 3D and three benchmark problems from the literature with high absorption.

Keywords: convective transport, convection–diffusion–reaction, transient, finite element method, FIC, PFEM, Eulerian, Lagrangian.

1. Introduction

The convective transport of a physical quantity such as heat or a chemical concentration accounting for diffusion and absorption effects is a phenomenon that plays a central role in many applications of interest. Such phenomenon is well described by a differential equation of an advection-diffusion-absorption type. A large volume of scientific work has been devoted to the study of this equation and, in particular, to its solution by numerical means. The problem is well-studied for a variety of methods like finite differences [13], finite volumes [32] and the finite element method (FEM) [10, 11, 18, 21, 35, 36], among others. Nonetheless, this numerical problem remains a challenging one, especially for high Péclet numbers, due to the difficulty of accurately representing three processes (advection,

diffusion and absorption) when their corresponding time and space scales are very different for some particular classes of problems.

Transport problems involving high-Péclet numbers (Pe) are common in many practical situations. Among these, we note the study of environmental pollution, either related to the quality of air or water,[6] or the simulation of the advection-diffusion in a microfluidics channel [34], just to name a few.

Standard FEM techniques for solving convective transport problems based on the Eulerian description of the continuum suffer from instabilities if not endowed with the appropriate stabilization techniques [5, 23, 31]. These techniques, which are based on the addition of artificial diffusion terms, tend to spoil the accuracy of the numerical solution in cases where there is a (relatively small) physical diffusion. Thus, one is faced with a trade-off between stability and accuracy that is particularly restrictive for high-Péclet flows.

The numerical solution to the advection, diffusion and absorption problem is prone to exhibit global, Gibbs and dispersive oscillations, which require the application of specific stabilization techniques to control instabilities. The local Gibbs oscillations appear along the characteristic layers in advection-dominated problems. For absorption-dominated cases, Gibbs oscillations can be found near the Dirichlet boundaries and in regions where the distributed source term is nonregular. Also, the solution of the transient problem may exhibit dispersive oscillations when the initial solution and/or the distributed source term are nonregular [64]. Various techniques for solving these problems can be found in literature, such as the Petrov-Galerkin method [5, 23, 24, 31, 33], the Galerkin Least Squares (GLS) method [17, 25], the Variational Multiscale (VMS) method [26] or the characteristic split procedure [75, 77]. In this paper we will use the Finite Increment Calculus (FIC) stabilization technique which has been widely used to solve problems involving quasi and fully incompressible fluids and solids with the FEM [40, 41, 9, 48, 54, 49, 50]. The FIC technique is based on expressing the equations of balance of mass and momentum in a space/time domain of finite size and retaining higher-order terms in the Taylor series expansion used for expressing the change in the transported variables within the balance domain. In addition to the standard terms of infinitesimal theory, the FIC form of the balance equations contains derivatives of the classical differential equations multiplied by characteristic distances in space and/or time [40, 41, 50, 49, 54, 48].

In the last decades, various authors have investigated ways of solving transient prob-

lems for high-Péclet numbers. For instance, Sevilla et al. [68] studied the influence of the number of integration points in the accuracy of the computations, using high-order curved finite elements and proved that they were one order of magnitude more precise than classical isoparametric FEM. In [69], the simulation of dispersing plumes and puffs was studied using a second-order closure model and a parameterized Eulerian approach.

From a different perspective, fully Lagrangian methods have been used for high-Péclet flows. For instance, in [66] good results for the convection-diffusion equations coupled to the incompressible flow equations were obtained using two Langrangian methods.

A third option that exploits the benefits of a combined Eulerian-Lagrangian method has been studied by other authors to solve problems such as advection-diffusion [7, 8, 38], the solute transport in heterogeneous porous media [67] or the nanoparticle distribution in nanofluids [2]. Many of these studies have proved that an splitting of an Eulerian and a Lagrangian solution can solve the excessive numerical diffusion observed in Eulerian methods. These splittings aim to accurately solve the advective part of the transport equation using a Lagrangian method and then calculate the diffusion problem via an Eulerian technique.

A combination of the Backwards Method of Characteristics with various Eulerian methods such as finite differences or finite elements was studied in [3]. Good results were obtained for high Courant numbers but no clear conclusion was reached on the stability and convergence of the methods. Cady [8] used a Modified Method of Characteristics together with finite differences and the Galerkin method but found accuracy problems. In the following years, the problem of global mass conservation due to the integration of the mass balance equation was addressed. In 1998, Healy and Russell [22] proposed the finite volume Eulerian-Lagrangian localized method with a forward tracking of the characteristics that lead to better results in comparison with previous methods. The performance of four Eulerian-Lagrangian solvers that relied on different interpolators was studied in [67]. It was found that the taut spline interpolator was able to yield accurate solutions for high-Péclet numbers. This method, based on a forward tracking algorithm, proved to be more efficient than other methods, such as the Petrov–Galerkin technique, for this kind of problems. The accuracy of the Petrov-Galerkin method can however be improved with the FIC stabilization [63, 65, 64]. In 2000 and 2006, respectively, Young et al. studied several Eulerian-Lagrangian methods such as the Eulerian-Lagrangian Boundary Element Method [73], which provided the solution for low numerical diffusion, and the Eulerian-

Lagrangian method of fundamental solutions [74], which is a mesh-free method that has the simplicity of a fixed grid from the Eulerian method and the computational power of the Lagrangian method. More recently, Wang et al. have studied a Eulerian-Lagrangian Discontinuous Galerkin Method [70, 71] and a Modified Method of Characteristics with an adjusted advection procedure [72] for the transient advection-diffusion equations. In 2012, Al-Lawatia [1] developed a mass conservative Eulerian-Lagrangian control volume scheme for the solution of the same equations in two dimensions (2D), based on the Eulerian-Lagrangian localized adjoint method [22].

Most of the works cited above employ an Eulerian-Lagrangian splitting for the advection-diffusion equation. In this work we present an alternative Eulerian-Lagrangian split formulation, termed *semi-Lagrangian formulation*, for the advection-diffusion-absorption equation that leads to accurate and stable results, and has neither convergence nor grid orientation problems. The Lagrangian part of the method is based on the Particle Finite Element Method - second generation (termed from here onwards PFEM2) [30, 27], which has been successfully used to simulate problems of sediment transport [4], diffusion dominant problems [20] and free surface flows [19], while the Eulerian formulation follows the FIC-FEM procedure presented in [65].

The semi-Lagrangian approach benefits from the FIC-FEM stabilized Eulerian method and the Lagrangian PFEM2 one. In the paper we will compare the benefits of the semi-Lagrangian method versus the standard Eulerian procedure for solving advection–diffusion–absorption problems.

The paper is organized as follows. First, the Eulerian solution scheme using a FIC-FEM procedure is introduced. Next, the PFEM2 technique is described and the Eulerian-Lagrangian splitting strategy is detailed. Several examples are presented in order to highlight the advantages of using the new semi-Lagrangian formulation versus the standard Eulerian approach: the evolution of a concentration field in a high-Péclet flow in 2D, the evolution of a spherical field in 3D and three advective-diffusive-absorptive problems.

2. Eulerian approach

In this section, we present the FIC-FEM Eulerian formulation for solving the multi-dimensional advection-diffusion-absorption equations. The procedure follows the recent work of the authors [65].

2.1. Governing equations

Transport balance

The transport balance equation in a domain of area/volume Ω is expressed as

$$r_t = 0 \quad \text{in } \Omega \tag{1a}$$

with

$$r_t := \rho c \left(\frac{\partial \phi}{\partial t} + \mathbf{v}^T \boldsymbol{\nabla} \phi \right) - \boldsymbol{\nabla}^T \mathbf{D} \boldsymbol{\nabla} \phi + s\phi - Q \tag{1b}$$

For 3D problems,

$$\mathbf{v} = \begin{bmatrix} v_1 \\ v_2 \\ v_3 \end{bmatrix}, \quad \mathbf{D} = \begin{bmatrix} k_1 & 0 & 0 \\ 0 & k_2 & 0 \\ 0 & 0 & k_3 \end{bmatrix}, \quad \boldsymbol{\nabla} = \begin{bmatrix} \partial/\partial x_1 \\ \partial/\partial x_2 \\ \partial/\partial x_3 \end{bmatrix} \tag{2}$$

In Equations (1a)–(1b)–(2) ϕ is the transported variable (i.e., the temperature in a heat transfer problem or the concentration in a mass transfer problem), v_i is the ith cartesian component of the velocity vector $\mathbf{v}$; ρ, c and k_i are the density, the specific flux parameter and the conductivity of the material along the ith global direction, respectively and s is the reaction parameter. In the following, and unless otherwise specified, we will assume that the problem parameters (ρ, c, k, s) are constant over the analysis domain Ω. In our work we define D = k/ρc as the normalized diffusivity, and R = s/ρc as the normalized absorption.

Boundary and initial conditions

The boundary conditions of the aforementioned equations are

$$\phi - \phi^p = 0 \quad \text{on } \Gamma_\phi \tag{3}$$

$$r_\Gamma = 0 \quad \text{on } \Gamma_q \tag{4}$$

with

$$\tag{5}$$

$$r_\Gamma := -q_n + q_n^p \tag{6}$$

where

$$q_n = \mathbf{q}^T \mathbf{n} \quad , \quad \mathbf{q} = -\mathbf{D}\boldsymbol{\nabla}\phi \tag{7}$$

In Equations (3)–(7) ϕ^p and q^p are the prescribed boundary fields of the transported variable and the outgoing diffusive flux at the Dirichlet and Neumann boundaries Γ_ϕ and Γ_q, respectively, with $\Gamma_\phi \cup \Gamma_q = \Gamma$, $\Gamma_\phi \cap \Gamma_q = \varnothing$, with Γ being the boundary of Ω and $\mathbf{n}$ its exterior unit normal.

The definition of the problem is completed with the *initial conditions*

$$\phi(\mathbf{x}, t_0) = \phi_0(\mathbf{x}) \tag{8}$$

where ϕ_0 is a known field.

2.2. Finite increment calculus (FIC) expressions

The governing equations (1a) and (1b) and the boundary conditions (3)-(7) are expressed using the FIC theory as [57].

Transport balance

$$r_t - \underline{\frac{1}{2}\mathbf{h}^T \boldsymbol{\nabla} r_t} = 0 \qquad \text{in } \Omega \tag{9}$$

with $\mathbf{h} = [h_1, h_2, h_3]^T$ in 3D.

Boundary conditions

$$\phi - \phi^p = 0 \quad \text{on } \Gamma_\phi \tag{10a}$$

$$r_\Gamma + \underline{\frac{1}{2} h_n r_t} = 0 \quad \text{on } \Gamma_q \quad , \quad \text{with } h_n = \mathbf{h}^T \mathbf{n} \tag{10b}$$

Equations (9) and (10b) are obtained by expressing the balance of fluxes in an arbitrary prismatic space domain of size $h_1 \times h_2 \times h_3$ within the global problem domain and at the Neumann boundary, respectively. The distances h_i are termed *characteristic lengths* of the FIC method. The variations of the transported variable within the balance domain are approximated by Taylor series expansions retaining one order higher terms than in the infinitesimal theory [40]. This higher-order expansions produce the underlined terms in Equations (9) and (10), which provide the necessary stability for the corresponding discretized equations.

Note that, as the characteristic length vector $\mathbf{h}$ tends to zero, the FIC governing equations tend to the standard infinitesimal form; that is, $r_t \to 0$ in Ω and $r_\Gamma \to 0$ on Γ_q as $\mathbf{h} \to \mathbf{0}$.

The characteristic lengths are small quantities which are defined in the context of the discrete problem and whose value influences the stability and accuracy of the method. In practice, they are expressed as a proportion of a typical grid dimension [40]. The characteristic length vector is defined in [65] as the sum of the streamline characteristic vector $\mathbf{h}_v$, the absorption characteristic length vector $\mathbf{h}_r$ and the shock capturing characteristic length vector $\mathbf{h}_{s_c}$, i.e.

$$\mathbf{h} = \mathbf{h}_v + \mathbf{h}_r + \mathbf{h}_{sc} \tag{11}$$

The FIC equations are the starting point for deriving different stabilized numerical methods. In combination with the Galerkin FEM, they yield the so-called FIC-FEM procedure [63, 64] which has been successfully applied to problems of convective transport, fluid and solid mechanics such as advection-diffusion [40, 43, 44, 52], diffusion-absorption and Helmholtz [16], advection-diffusion-absorption [53, 57], advection-diffusion-reaction [63], incompressible fluid flow [55, 56, 58, 60, 62], fluid-structure-interaction [46, 51, 59], particle-laden flows and standard and incompressible solid mechanics [48, 54, 61]. The FIC approach has also been applied to a variety of problems in mechanics using the meshless finite point method [39, 42, 45, 47].

2.3. Space and time integration

The system of equations 9-10 has been discretized in space with the FEM and in time using an implicit Generalized Trapezoidal rule[12, 76]. Detail of the finite element matrices and vectors of the discretized problem can be found in [65]. The solution for the nodal values at a time instant is found using an incremental iterative strategy as

$${}^{i}\mathbf{H}^{n}\Delta\boldsymbol{\phi} = -{}^{i}\mathbf{r}_t^n \tag{12}$$

where $\Delta\boldsymbol{\phi}$ is the increment of the nodal variables, $(\cdot)^n$ denotes values at time $t = t_n$, ${}^{i}(\cdot)$ denotes values at the ith iteration and

$${}^{i}\mathbf{H}^{n} = \frac{1}{\theta\Delta t}\mathbf{M} + {}^{i}\mathbf{K}^{n} + \mathbf{C} + \mathbf{S} \tag{13}$$

$$ {}^{i}\mathbf{r}_t^n := \mathbf{M}\dot{\boldsymbol{\phi}} + [{}^{i}\mathbf{K}^n + \mathbf{C} + \mathbf{S}]{}^{i}\boldsymbol{\phi}^{n+\theta} - {}^{i}\mathbf{f}^n \tag{14} $$

In Equations (13) and (14), θ is a non dimensional time parameter ($0.5 < \theta \leq 1$ is required for the integration scheme to be unconditionally stable [12, 76, 77]).

The non-linearity of $\mathbf{K}$ is due to its dependance with ϕ when the equations are stabilized with the FIC procedure [65].

In Equation (14) we define $\dot{\boldsymbol{\phi}} = \frac{\boldsymbol{\phi}^{n+\theta} - \boldsymbol{\phi}^n}{\theta \Delta t}$.

From the value of $\Delta\boldsymbol{\phi}$ obtained from Equation (12) we compute the value of $\boldsymbol{\phi}^{n+\theta}$ at the $i+1$ iteration as

$$ {}^{i+1}\boldsymbol{\phi}^{n+\theta} = {}^{i}\boldsymbol{\phi}^{n+\theta} + \Delta\boldsymbol{\phi} \tag{15} $$

The iterative solution at t_{n+1} is obtained as

$$ {}^{i+1}\boldsymbol{\phi}^{n+1} = \frac{1}{\theta}{}^{i+1}\boldsymbol{\phi}^{n+\theta} + \left(1 - \frac{1}{\theta}\right)\boldsymbol{\phi}^n \tag{16} $$

The iterations proceed until convergence is achieved for both the unknown field ϕ and the residual $\mathbf{r}_t$ measured in a L_2 norm. A detailed explanation of each component of Equations (13) and (14) can be found in [65].

3. Semi-Lagrangian approach

Although good results were obtained in [65] when solving the advection-diffusion-absorption equations, it was observed that excessive diffusion was obtained for problems involving high-Péclet numbers. This was the motivation for using the Lagrangian PFEM2 [27] to solve this type of problems, in view of its particular feature of non adding numerical diffusion for the advective problem. PFEM2 can be understood as a splitting method, which uses a set of particles to solve the pure convective transport problem and a finite element mesh to solve the rest of the transport equations. In our work the PFEM2 is used to solve the advection equation. Following that, the diffusion-absorption equations are solved with the FIC-FEM Eulerian strategy.

Let us start by rewriting the transport balance Equation (1b) using the total time derivative as

$$ r_t := \rho c \frac{D\phi}{Dt} - \nabla^T \mathbf{D} \nabla\phi + s\phi - Q = 0 \tag{17a} $$

$$ \frac{D\mathbf{x}}{Dt} = \mathbf{v} \tag{17b} $$

Equation (17a) can be integrated using the trapezoidal rule explained in Section (2.3). Due to the dependence with Equation (17b), a coupling between the time integration of both equations shall be defined.

3.1. Advection step

Let us define a set of particles in the same domain as the finite element space, where each particle stores the point concentration of the property $\phi_p = \phi(\mathbf{x}_p)$. Since the variables are not known for any arbitrary time t, but only for the discrete time steps $1,\ 2 \dots n,\ n+1 \dots$ defined in Section (2.3), the advection of a particle can be approximated using a θ-family discretization as:

$$\mathbf{x}_p^{n+1} = \mathbf{x}_n^p + (1-\theta)\int_{t_n}^{t_{n+1}} \mathbf{v}_n(\mathbf{x}_p^t)dt + \theta\int_{t_n}^{t_{n+1}} \mathbf{v}_{n+1}(\mathbf{x}_p^t)dt \tag{18}$$

If the velocity field is known, the system becomes explicit and the problem is reduced to moving the particles along the streamlines. The problem is solved using an explicit forward integration ($\theta = 0$) with substepping [30]. This method, also known as XIVAS [29][28], was initially applied to a variable velocity field.

3.2. Projection

When solving the advective step in Equation (17a), the particles concentration at $\mathbf{x}_p^{n+1}$ is the same as at the onset of the time step ($\mathbf{x}_p^n$). This is equivalent to say that the advective step assumes $\frac{D\phi}{Dt} = 0$. This modification in the field described by the particles needs to be transferred into the finite element space. As usual in particle-based techniques, such as PFEM, a projection procedure is used to transfer the information from the particles to the finite elements in the underlying mesh. In our work we use

$$\phi^* = \mathcal{L}(\phi_p) \tag{19}$$

where $\mathcal{L}$ is the projection operator from the particles to the finite element space and ϕ^* is the result of the advection at the time step $n+1$. In this case, a first order explicit projection has been used and all the particles in the elements surrounding a node contribute to that node, i.e.

$$\phi_i^* = \frac{\Sigma_e \Sigma_{p_e} w_p \phi_p}{\Sigma_e \Sigma_{p_e} w_p} \quad \text{with} \quad w_p = N_{ei}(\mathbf{x}_p) \tag{20}$$

where i denotes the node and e the elements sharing the node.

3.3. Diffusion-absorption stage

Once the advection problem is solved explicitly in the particles and the results are transferred to the mesh nodes, the lagrangian residual (Equation (17a)) is solved in a fixed grid with a FIC-FEM Eulerian technique. The spatial discretization and the time integration scheme follows the procedure explained in Section (2.3). Details are given in [65].

Note that the advective term $\mathbf{C}$ from Equation (14) vanishes as advection is modelled with the Lagrangian approach and the time derivative $\dot{\phi}$ denotes now the total derivative (Equation (17a)).

The total time derivative is computed as

$$\dot{\phi} = \frac{\phi^{n+\theta} - \phi^*}{\theta \Delta t} \tag{21}$$

Equation (21) includes the contribution of the advection computed with the particles.

As explained in Section 3.1, the advection is calculated separately from the diffusion and the absorption with the PFEM2 procedure. As the equations solved with an Eulerian approach are free from advective instabilities, this splitting simplifies the equations in the following way. The parameter $\mathbf{h}_v$, which helps solving global advective instabilities is set to zero as the advection is calculated through a particles method. $\mathbf{h}_{sc}$, which is used to attenuate Gibbs oscillations that appear along characteristic layers is also set to zero as these oscillations do not appear in the PFEM2 method. Finally, the advective components of $\mathbf{h}_r$, are set to zero as the velocity is computed in previous steps and does not intervene in the diffusion-absorption stage. The characteristic length parameter from Equation (11) needed for the FIC–FEM Eulerian solution is then computed as

$$\mathbf{h} = \mathbf{h}_r = \frac{2}{r_t} \mathbf{D_s} \nabla \phi \tag{22}$$

where matrix $\mathbf{D}_s$ takes care of the instabilities induced by the irregularity of the triangular mesh near boundaries that develop parabolic layes [64].

The new characteristic length (Equation (22)) leads to the disappearance of the non-linearity seen in Equations (13) and (14), which simplifies the resolution of the advection-diffusion-absorption equation.

3.4. Particles update

The last step of the PFEM2 algorithm is to add the contribution of the solution of Equation (17a) to the particles. To avoid the accumulation of projection errors and additional diffusion, the information from the particles is updated using an incremental scheme. This step only involves the evaluation of the unknown at each particle position in the finite element mesh as:

$$\phi_p^{n+1} = \phi_p^n + \phi(\mathbf{x}_p^{n+1}) - \phi(\mathbf{x}_p^*) \tag{23}$$

The basic steps of the PFEM2 procedure can be seen in Figure 1.

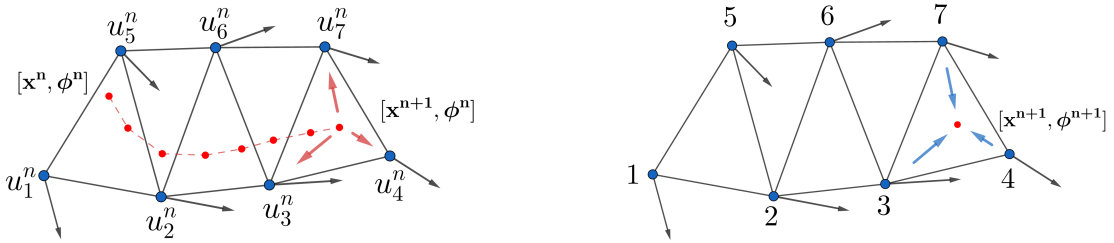

(a) Explicit advection stage using particles (in red). Next, the particles' information is transferred to the mesh nodes (in blue).

(b) Diffusion-absorption stage. Contribution of the finite element nodes to the particles.

Figure 1: Illustration of the two main steps of the PFEM2 framework.

Properties of the PFEM2 procedure

Apart from removing the numerical diffusion added from the FEM Eulerian approach, PFEM2 has proven to be very accurate when large time-steps and/or coarse meshes are used [27]. However, due to the projection of the information, as well as the updating of the particles, the method does not guarantee mass conservation. In Section 4.1 we integrated the concentration value to assess the algorithm's mass conservation in the domain after 15 s of simulation and we observed negligible mass changes. This is distinct feature of PFEM [50] and will be studied in further publications. Also, the semi-Lagrangian method removes non-linearities, as explained in Section 3.3.

4. Examples

We present five examples of application of the semi-Lagrangian formulation: the transport of a concentration of a solute in a fluid domain (both in 2D and 3D) and three

advective–diffusive–absorptive problems.

4.1. 2D transport of a concentration

4.1.1. Introduction

We study the evolution of an initially point-like concentration of solute as it is transported and diffused from a point source in a fluid with a known velocity field. The main interest is to compare the accuracy of a purely Eulerian approach versus the semi-Lagrangian method previously described from low to very high Péclet numbers.

We will consider a uniform velocity field parallel to the x-axis of 1 m/s. Two different values will be considered for the diffusivity: $D = 0.1$ m^2/s for the low-Péclet ($Pe = 2.5$) example and $D = 0$ m^2/s for the high-Péclet one ($Pe \to \infty$). The Péclet number is defined as follows: $Pe = \frac{ul}{2D}$, where u is the horizontal velocity, l is the characteristic length and D is the normalized diffusivity. The examples have been run with $\rho c = 1$ J/m^{3}K. The analysis domain $(x, y) = [0, 35] \times [0, 10]$ m is discretised in a regular mesh of 3-noded triangles with a characteristic length $l = 0.5$ m, which gives us a domain of $2 \times (70 \times 20)$ elements.

The Dirichlet boundary condition $\phi = 0$ kg/m^2 at $x = 0$ m and the initial concentration $\phi(x_0, y_0, 0) = 1000$ kg/m^2 at $\mathbf{x}^0 = (2, 5)$ m are considered. Figure 2 shows a diagram of the whole set-up (note that the point $(2, 5)$ is made to coincide with a mesh node).

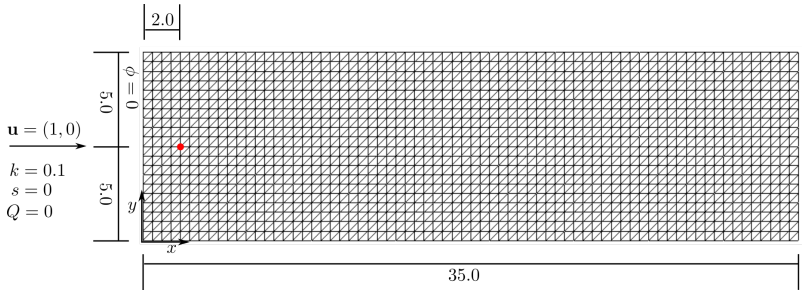

Figure 2: 2D transport of a concentration. Finite element mesh. The initial concentration is depicted in red at point (2, 5)

For the numerical solution, the initial condition is defined by the value of the concentration at a single node ($\phi_0 = 1000$ kg/m^2 at node (2, 5), 0 everywhere else) as a single shape function whose maximum concentration coincides with ϕ_0. This corresponds to a total mass of 250 kg for the numerical simulation.

The numerical solution is compared to an analytical solution that consists in the transport and diffusion of a Gaussian density distribution [37]. The initial conditions in this

case are defined as

$$\phi(x,y,t) = \frac{\phi_0}{L_3 4\pi D\hat{t}} e^{-A} \tag{24a}$$

with

$$A = \frac{1}{4D\hat{t}} \left\{ [x_1 - (x_1^0 + u_1(\hat{t} - t^0))]^2 + [x_2 - (x_2^0 + u_2(\hat{t} - t^0))]^2 \right\} \tag{24b}$$

where t^0 is calculated such that at $\hat{t} = t^0$, ϕ corresponds to a Gaussian whose height is equal to 1000 kg/m^2 and is centered at the node (2, 5) and such that the initial total mass coincides with the one imposed as the initial condition in the numerical solution.

ϕ_0 is the initial value of the mass that is dropped at $\mathbf{x}^0$ and $t = \hat{t} - t^0 = 0$ s, which can lead to small discrepancies in the results as there is a slight inaccuracy in the definition of the initial conditions, although this difference will dissipate exponentially in time.

L_3 is the vertical dimension of the analysis domain (we have taken $L_3 = 1$), u_1 and u_2 are the horizontal and vertical components of the velocity vector and D is the normalized diffusivity. In all cases, the density ρ and the specific flux c are chosen such that $\rho c = 1$ J/m^{3}K. We have also assumed an isotropic diffusion. Several cases have been studied to see the effect of the advective and diffusive terms on the result.

The time-integration parameters are chosen as $\theta = 0.5$ and $\Delta t = 0.5$ s. Taking into account these parameters the Courant number is $C = 1$.

4.1.2. Results

The results obtained with the Eulerian and the semi-Lagrangian methods are presented next.

- Eulerian and semi-Lagrangian solutions for $Pe = 2.5$

  We have compared the Eulerian and semi-Lagrangian solutions with the analytical one. Numerical results show a slight difference of concentration versus the analytical values. While in the Eulerian method a maximum concentration value of 13.234 kg/m^2 is obtained, using the semi-Lagrangian approach this value is 13.085 kg/m^2. The maximum analytical value for the same case at $t = 15$ s is $\phi = 13.089$ kg/m^2 (Figure 3e), which represents a percentual gain of 1.11% in the Eulerian case (Figure 3a) and 0.03% loss in the semi-Lagrangian one (Figure 3c). In both cases, the

concentration difference is small and thus we can conclude that both methods work well for this Péclet number.

Looking at the concentration contour at Figure 3a, we can observe a small deformation of the resulting shape for the Eulerian case due to the slightly higher numerical diffusion.

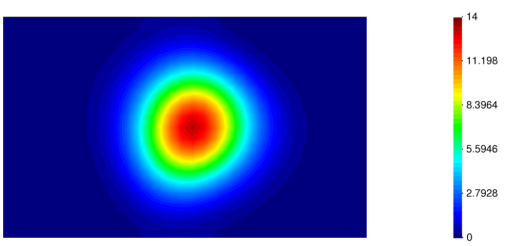

(a) Eulerian solution for $Pe = 2.5$.

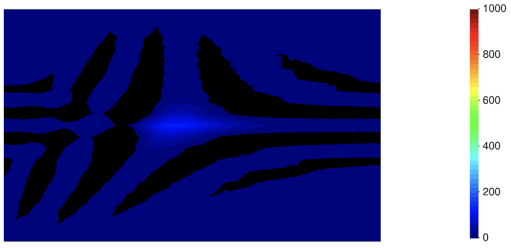

(b) Eulerian solution for $Pe \to \infty$.

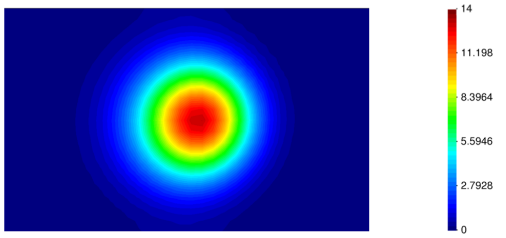

(c) Semi-Lagrangian solution for $Pe = 2.5$.

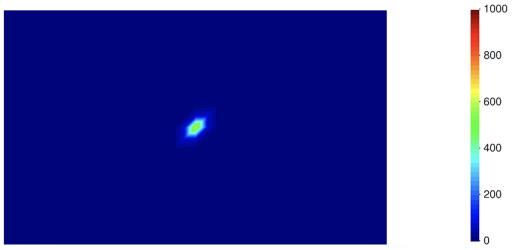

(d) Semi-Lagrangian solution for $Pe \to \infty$.

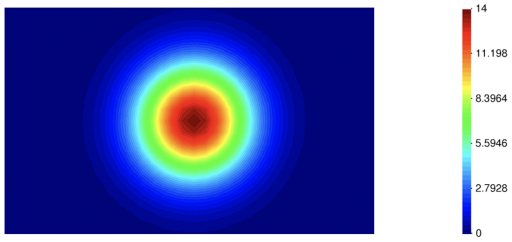

(e) Analytical solution for $Pe = 2.5$.

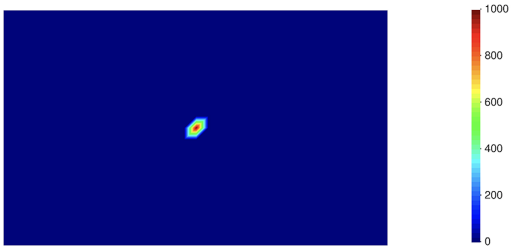

(f) Analytical solution $Pe \to \infty$.

Figure 3: 2D transport of a concentration. Eulerian, semi-Lagrangian and analytical results compared at $t = 15s$.

- Eulerian and semi-Lagrangian solutions for $Pe \to \infty$

  In this case, the effect of the diffusive component vanishes. The Eulerian result in Figure 3b shows a solution which is not representative of the analytical one and keeps on diffusing as the simulation advances. On the other hand, the semi-Lagrangian result in Figure 3d, shows a concentration transport without any loss in time, as in the analytical solution for the same Pe (Figure 3f). The maximum value of the semi-Lagrangian method is 626.55 kg/m^2, which corresponds to the projection of the

maximum concentration on the mesh from the particles, that is, there is a diffusion towards the adjacent elements from the point where the concentration is assigned. The sum of the concentrations on these adjacent elements coincides with the initial maximum value of 1000 kg/m^2.

4.1.3. Sensitivity analysis

In this subsection we run several cases varying the value of the diffusivity between the lowest and highest Péclet number of the examples (from $Pe = 2.5$ to $Pe \to \infty$).

Table 1 presents the maximum concentration values for each of the methods with different diffusivities. The reference values obtained with the analytical solutions are included for comparison.

		Maximum concentration value [kg/m^2]		
		Analytical	*Semi-Lagrangian*	*Eulerian*
Pe	$\to \infty$	1000.00	626.55	129.92
	2.5e06	999.92	626.53	129.92
	2.5e05	999.25	626.36	129.90
	2.5e04	992.52	624.61	129.73
	2.5e03	929.89	607.60	128.03
	2.5e02	570.131	470.390	113.910
	2.5e01	117.098	118.130	65.081
	4.55	23.570	25.835	24.687
	3.33	17.360	17.372	17.410
	2.50	13.089	13.085	13.234

Table 1: 2D transport of a concentration. Maximum concentration values of each method in different values of Péclet.

Clearly, the semi-Lagrangian approach, which benefits from the particle Lagrangian motion, works very well for purely advective as well as for the range of Péclet numbers considered in this study.

On the other hand, we observe that the Eulerian FIC-FEM method solves stability problems, especially in the most diffusive cases. The solutions coincide with the semi-Lagrangian results.

Figure 4 shows the maximum concentration in terms of the Péclet number. Note how the Eulerian approach presents a huge numerical diffusion for high-Péclet numbers. The

semi-Lagrangian approach provides more accurate results. The difference between the analytical solution and the semi-Lagrangian results is assessed in Section 4.1.4.

Note that for $Pe \lesssim 2.5$, the Eulerian solution begins to gain relevance and the results are comparable to those obtained with the semi-Lagrangian approach.

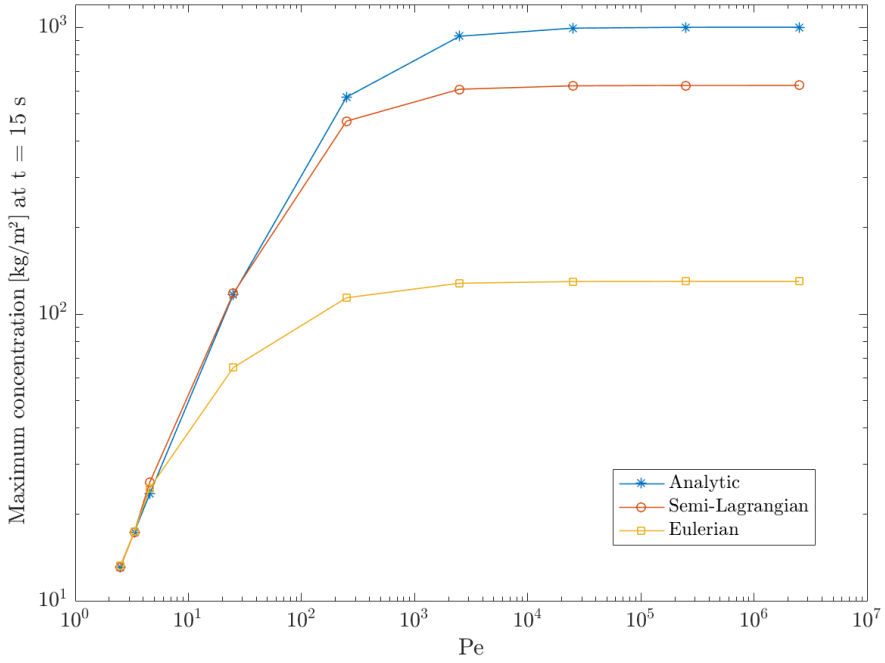

Figure 4: 2D transport of a concentration. Comparison of the analytical, semi-Lagrangian and Eulerian methods in terms of the Péclet number.

4.1.4. Numerical diffusion analysis

This section studies the examples of Section 4.1.2, which are now plotted along time to see their relative impact in the numerical diffusion.

Figure 5 shows that, although the first four seconds of the example differ slightly, the results are quite identical at t = 15 s.

The example with $Pe \to \infty$ is shown in (Figure 6). We can see that the semi-Lagrangian method presents no diffusion loss whatsoever in the maximum transported value, except from that introduced by the projection of the nodal concentration to the adjacent elements.

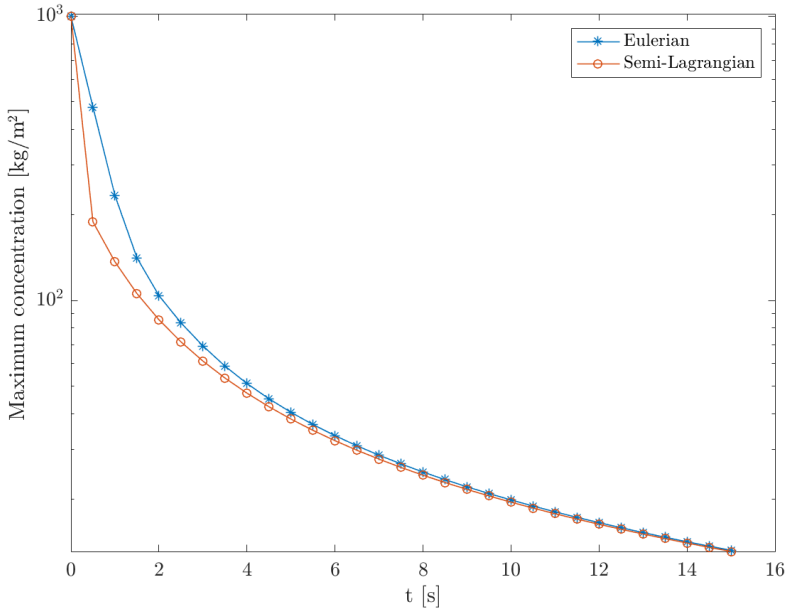

Figure 5: 2D transport of a concentration. Comparison of the maximum transported value from t = 0 s to t = 15 s using the semi-Lagrangian and Eulerian methods ($Pe = 2.5$).

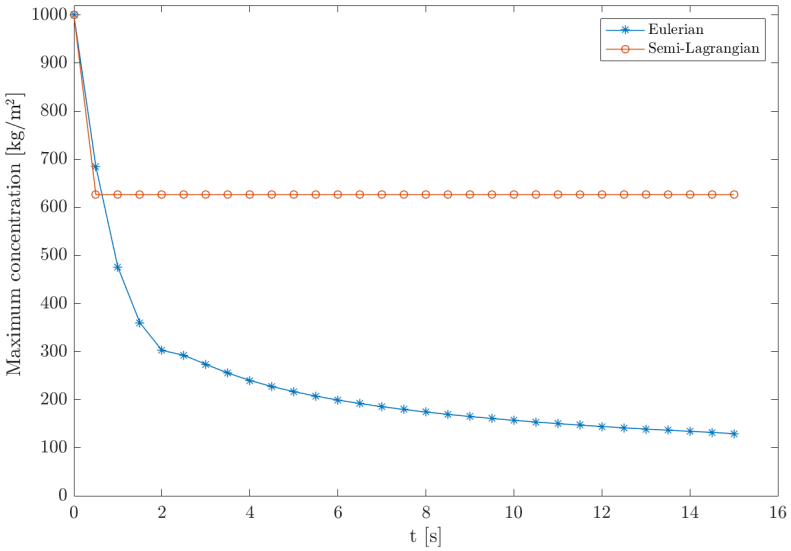

Figure 6: 2D transport of a concentration. Comparison of the maximum transported value from t = 0 s to t = 15 s using the semi-Lagrangian and Eulerian methods ($Pe \to \infty$).

4.2. Pure 3D advection of a spherical concentration

A 3D problem equivalent to the point concentration in 2D has been studied in this section. It consists in the pure advective transport ($Pe \to \infty$) of a uniform spherical

blob of concentration. The spherical blob has a radius of 0.8 m and is initially centered at $(x, y, z) = (2.5, 2.5, 2.5)$. The computational domain is the extruded version of the one considered in the previous 2D example, with a velocity of 1 m/s along the x-axis, a normalized diffusivity $D = 0.0$ m^2/s and a normalized absorption $R = 0.0$ s^{-1}. The analysed domain $(x, y, z) = [0, 15] \times [0, 5] \times [0, 5]$ m is discretised into a regular mesh of $(150 \times 50 \times 50)$ 4-noded linear tetrahedra. The schematics of the problem are shown in Figure 7. A middle section of the volume at $t = 0$ s can be seen in Figure 8a.

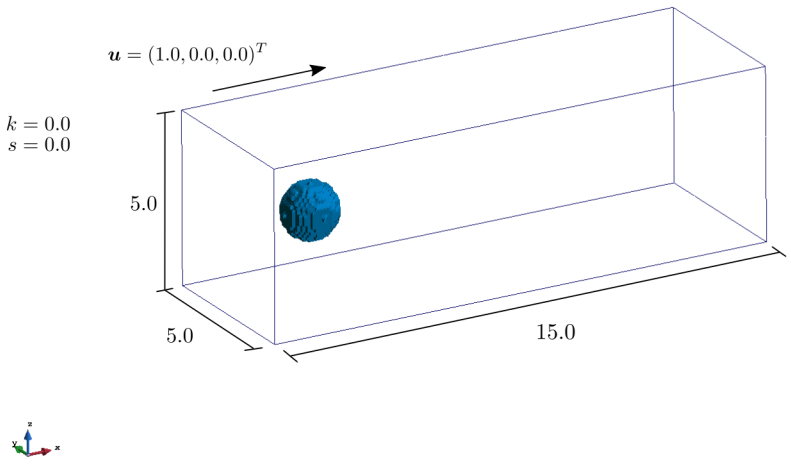

Figure 7: Sphere transportation problem set-up.

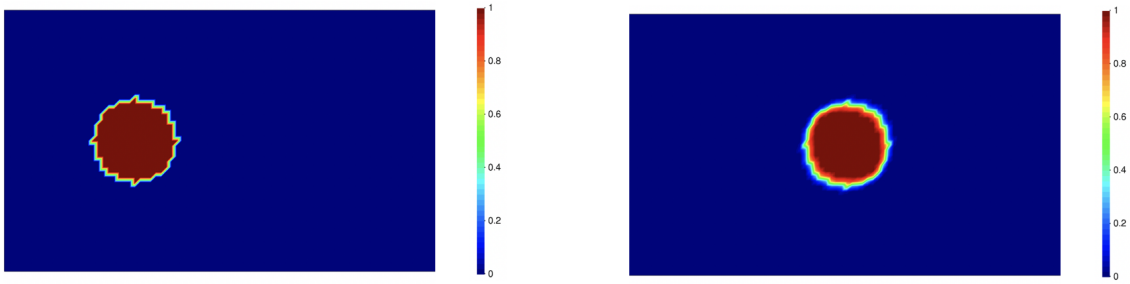

(a) Middle volume section at $t = 0$ s. **(b)** Sphere transport at $t = 5$ s.

Figure 8: Sphere transport. Middle plane cut from $t = 0$ s to $t = 5$ s ($Pe \to \infty$).

The results at $t = 5.0$ s show no concentration loss except from the one derived from the projection of the particles to the elements in the first step (Figure 8b).

In Figure 9 a 3D view of the transported sphere can be seen.

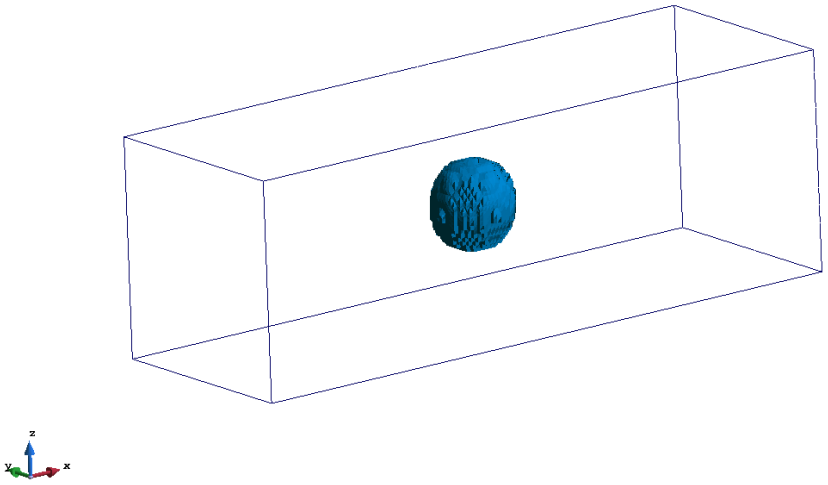

Figure 9: 3D view of the sphere at $t = 5$ s.

4.3. Transient advection–diffusion–absorption problem with sharp boundary layers

The analysis domain $(x, y) = [0, 8] \times [0, 8]$ is discretised into a regular mesh of $2 \times (8 \times 8)$ 3-noded triangles of unit rectangular side ($l = 1$) (Figure 10). The advection, diffusion and absorption coefficients are chosen as $u = 8$ m/s, $D = 2$ m^2/s and $R = 2.0$ s^{-1}. The transported variable is the mass, in Kg and $\rho c = 1$ J/m^{3}K. The schematics of the problem can be seen in Figure 10. The problem data yields a Péclet number of $Pe = 2.0$ and a Damköhler number of $Da = 150.0$. The Damköhler number is defined as $Da = \frac{sl}{u}$, where s is the reaction parameter, l is the characteristic length and u the velocity.

The Dirichlet boundary conditions $\phi(x = 0) = 3$ and $\phi(x = 8) = 8$ are employed. The initial solution is chosen to have a linear profile. The transient solution was obtained with the implicit iterative scheme explained in Section (2.3) with $\theta = 1.0$ and a time step of $\Delta t = 0.0625s$. This corresponds to an element Courant number $C = 0.5$. An exponential layer gradually develops at the right boundary which is attenuated thanks to the absorptive stabilization introduced by the FIC procedure (Figure 11).

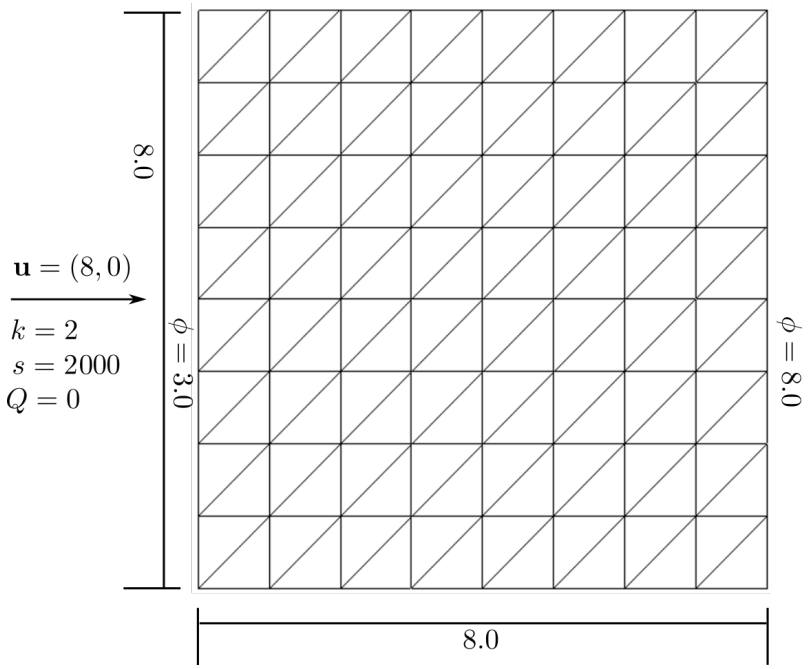

Figure 10: Transient advection–diffusion–absorption problem. Square domain with linear velocity and zero source.

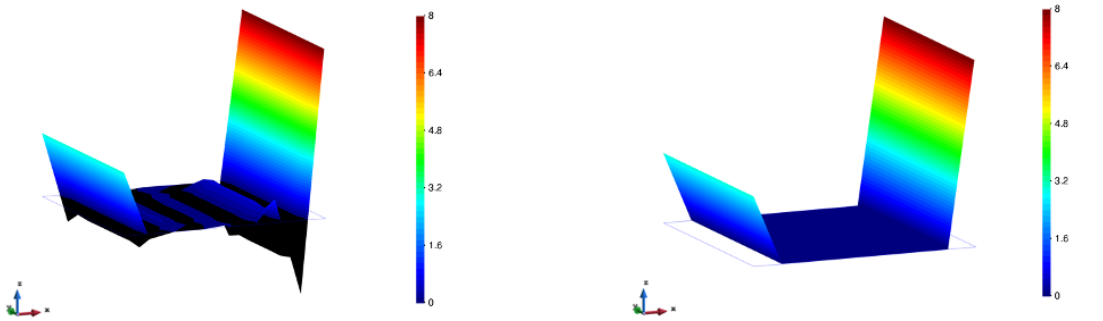

(a) Result without absorption stabilization.

(b) Result with absorption stabilization.

Figure 11: Transient advection–diffusion–absorption with sharp boundary layer. Results at $t =$ 2 s.

4.4. Transient advection-diffusion-absorption problem with a manufactured solution

This example consists in solving a low-diffusive advective-absorptive problem using the manufactured solution stated in Equation (25). This problem was solved by Duan et al. [14, 15].

$$\phi(x,y) = \left(\frac{x^2}{2u_1} + \frac{Dx}{u_1^2}\left(\frac{1}{2u_1} + \frac{D}{u_1^2}\right) \frac{\exp\frac{-u_1}{D} - \exp\left[\frac{-u_1}{D}(1-x)\right]}{1-\exp\frac{-u_1}{D}} \right) \times \left(\frac{y^2}{2u_2} + \frac{Dy}{u_2^2}\left(\frac{1}{2u_2} + \frac{D}{u_2^2}\right) \frac{\exp\frac{-u_2}{D} - \exp\left[\frac{-u_2}{D}(1-y)\right]}{1-\exp\frac{-u_2}{D}} \right) \tag{25}$$

Introducing Equation (25) into Equation (1b) yields the non-homogeneous source-like term Q that is used, in turn, to solve the advective–diffusive–absorptive equation with the semi-Lagrangian procedure.

We will consider a uniform velocity field of $\mathbf{u} = (u_1, u_2)^T := (1/2, \sqrt{3}/2)^T$. A value of D = 1e-2 m^2/s and R $= s/\rho c = 10^i$ 1/s with $i = 2, 3, 4$ have been taken.

These cases have been run with ρc = 1 J/m^{3}K. The analysis domain $\Omega := (x, y) = [0, 1] \times [0, 1]$ m is discretised in a regular mesh of $2 \times (1/2^i \times 1/2^i)$ 3-noded triangles with a characteristic length $l = 1/2^i$ m, being $i = 5, 6, 7, 8$.

A Dirichlet boundary condition of $\phi = 0$ kg at the whole boundary is considered. The time-integration parameters are chosen as: θ = 1.0 and Δt = 1e-4 s.

An image of the numerical result and the exact solution can be seen in Figure 13. Excellent agreement is obtained.

Table 2 shows the Damköhler numbers corresponding to each of the cases considered in the study.

Table 3 shows the root-mean-square error for each case analyzed. Taking the last two values (belonging to the finest mesh examples), the convergence has also been calculated.

	Damköhler numbers			
	R = 100 1/s	R = 1000 1/s	R = 10000 1/s	Péclet numbers
l = 1/32 m	3.13	31.25	312.50	1.56
l = 1/64 m	1.56	15.63	156.25	0.78
l = 1/128 m	0.78	7.81	78.13	0.39
l = 1/256 m	0.39	3.91	39.06	0.20

Table 2: Manufactured advective-diffusive-absorptive problem. Damköhler and Péclet numbers for each of the cases studied.

Figure 12 displays a graph of the results of Table 3.

	RMSE		
	R = 100 1/s	R = 1000 1/s	R = 10000 1/s
l = 1/32 m	0.00906573	0.00842561	0.00836711
l = 1/64 m	0.00420981	0.00370434	0.00362029
l = 1/128 m	0.00153896	0.00127547	0.00122659
l = 1/256 m	0.00056077	0.00038503	0.00036025
Convergence order	1.46	1.73	1.77

Table 3: Manufactured advective-diffusive-absorptive problem. Root-mean-square error (RMSE) and order of convergence for different values of R = s/ρc.

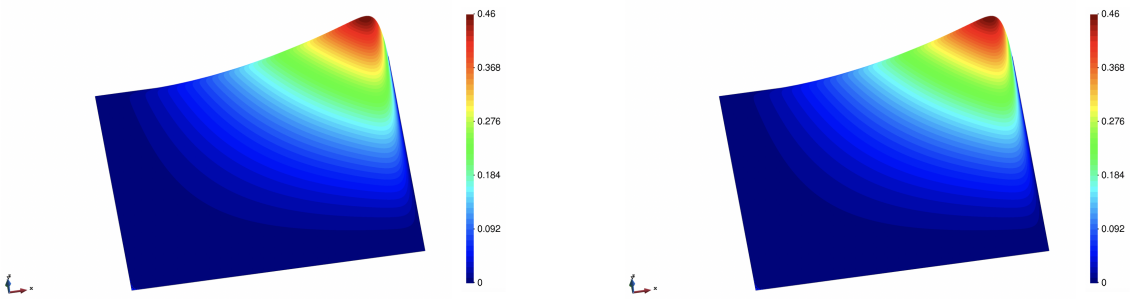

(a) Numerical solution. **(b)** Analytical solution.

Figure 13: Advective-diffusive-absorptive problem with manufactured solution. Elevation plot at $t = 0.08$ s with a $h = 1/256$, $D =$ 1e-2 m^2/s and a $R = 10^4$ 1/s giving $Pe = 0.20$ and $Da = 39.06$.

4.5. Manufactured transient advection–diffusion–absorption hump problem

This last example, taken from [14], consists in a hump moving in a domain changing its height periodically leading to the appearance of a strong interior layer adjacent to the hump walls. The exact solution is given by Equation (26). This solution is introduced into Equation (1b) to yield the manufactured unhomogeneous source-like function Q used for solving the advection-diffusion-absorption equation with the semi-Lagrangian procedure.

$$\phi(t,x,y) = 16\sin(\pi t)x(1-x)y(1-y) \times \left(\frac{1}{2} + \frac{\arctan[2\varepsilon^{-1/2}(0.25^2 - (x-0.5)^2 - (y-0.5)^2)]}{\pi}\right) \tag{26}$$

We have considered a uniform velocity field of $\mathbf{u} = (2,3)^T$. A value of $D =$ 1e-6 m^2/s has been chosen for the normalized diffusivity and $R = 1000$ 1/s for the normalized absorption.

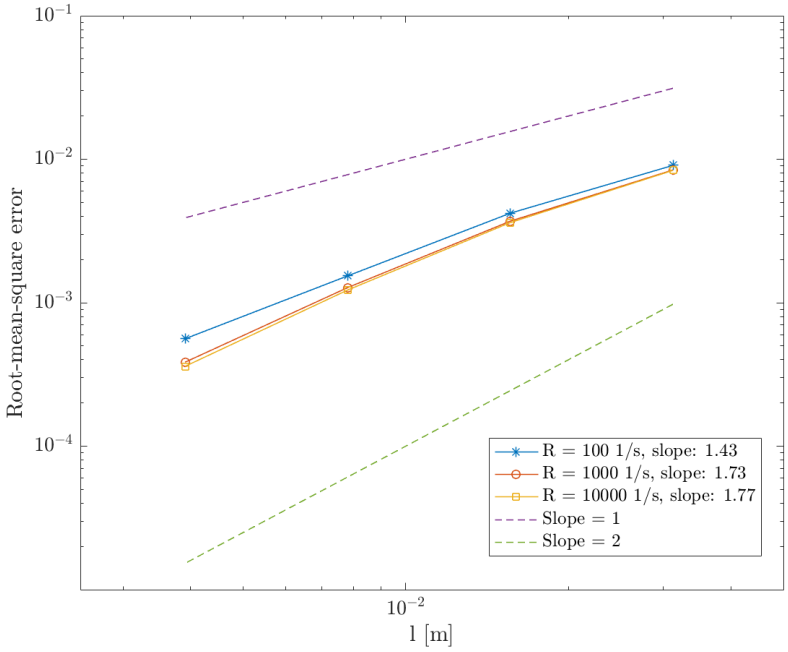

Figure 12: Manufactured advective-diffusive-absorptive problem. Root-mean-square error versus the characteristic length l. Lines with slope = 1 and 2 are plotted for reference.

These cases have been run with $\rho c = 1$ J/m^{3}K. The analysis domain $\Omega := (x, y) = [0, 1] \times [0, 1]$ m is discretised in a regular mesh of $2 \times (64 \times 64)$ 3-noded triangles with a characteristic length $l = 1/64$ m.

A Dirichlet boundary condition $\phi = 0$ kg at $\partial\Omega$ has been considered. The initial condition is $\phi = 0$ kg at $t = 0$ s. The time-integration parameters are chosen as: $\theta = 0.8$ and $\Delta t =$ 1e-3 s.

Results of the simulation can be seen in Figure 14.

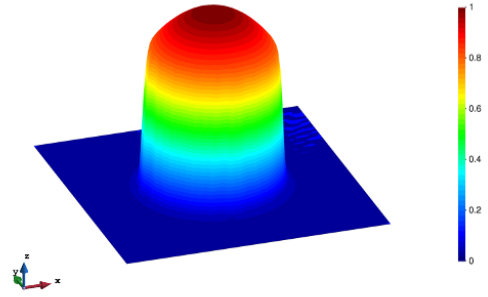

(a) Numerical solution.

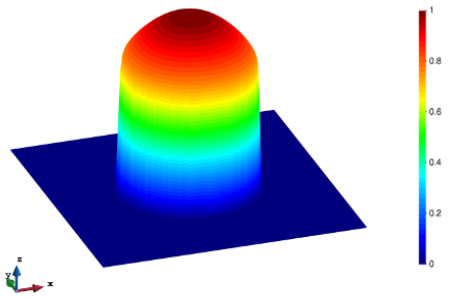

(b) Analytical solution.

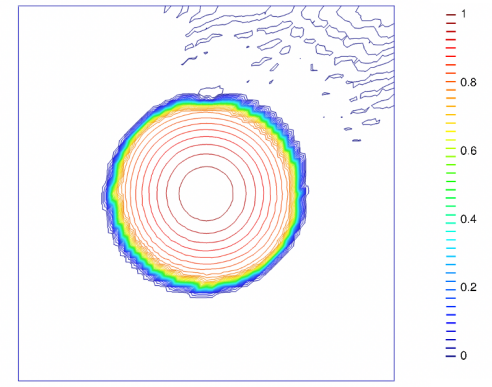

(c) Top view of the numerical solution.

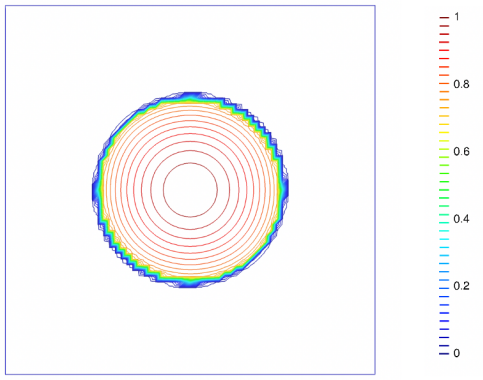

(d) Top view of the analytical solution.

Figure 14: Manufactured hump problem. Hump geometry at $t = 0.5$ s with $h = 1/64$, $D =$ 1e-6 m^2/s and $R = 1000$ 1/s, which corresponds to $Pe =$ 1.56e4 and $Da = 15.63$.

The results show that the solution is stable and does not exhibit spurious oscillations near the interior layer region. Some minor oscillations – $\approx 2\%$ of the maximum value – can be spotted on the top-right side of the domain.

A qualitative comparison with the examples in [14] shows that the semi-Lagrangian procedure is highly competitive with the best methods in that paper.

5. Concluding remarks

We have presented numerical method that combines a FIC-FEM stabilized Eulerian procedure with a semi-Lagrangian PFEM2-based approach that splits the advection–diffusion–absorption equation into a combination of a pure advective problem and a diffusive-absorptive one. The goal is the solution of advection-diffusion-absorption transport problems at high-Péclet and high-Damköhler numbers.

The presented method involves a more complex algorithm than the one in [65] but re-

moves the non-linearity introduced by the previous stabilization. Low numerical diffusion is achieved due to the use of a Lagrangian method in the advection step. However, mass conservation in the domain is not guaranteed.

We first solved a 2D pure transport example to assess the behaviour of the mixed formulation when compared to an Eulerian one from advection-dominated cases to highly diffusive ones. The results show that, although the Eulerian base formulation behaves well for highly diffusive problems, it fails to accurately transport the heat / mass concentration in problems with high-Péclet numbers ($Pe > 5.0$) due to the high numerical diffusion introduced by the formulation. In contrast, the semi-Lagrangian approach remains accurate, without any numerical loss, even for $Pe \to \infty$.

We also have solved the transport of a sphere of heat / mass concentration and verified that the semi-Lagrangian approach is just as accurate for 3D problems.

After that, we studied three problems with higher Damköhler numbers in order to verify that the semi-Lagrangian method gives accurate and stable results for highly absorptive problems.

The first of these examples showed the benefits of the absorption stabilization in a problem where a boundary layer develops at the boundary due to the effect of absorption. Furthermore, our proposed algorithm was tested using two complex benchmarks from the literature with known analytical solutions. Its performance was satisfactory in both cases, indicating that it is a very robust method, suitable for its use for the solution of general advection-diffusion-absorption problems.

Acknowledgements

This research was partially funded by the projects PRECISE (BIA2017-83805-R) and PARAFLUIDS (PID2019-104528RB-I00) of the Natural Research Plan of the Spanish Government. The authors also acknowledge the financial support from the CERCA programme of the Generalitat de Catalunya, and from the Spanish Ministry of Economy and Competitiveness, through the "Severo Ochoa Programme for Centres of Excellence in R&D" (CEX2018-000797-S).

References

[1] Al-Lawatia, M. An Eulerian-Lagrangian control volume scheme for two-dimensional unsteady advection-diffusion problems. *Numerical methods for partial differential*

equations 2012; **28(5)**:1481-1496.

[2] Bahiraei, M. Studying nanoparticle distribution in nanofluids considering the effective factors on particle migration and determination of phenomenological constants by Eulerian–Lagrangian simulation. *Advanced Powder Technology* 2015; **26(3)**: 802-810.

[3] Baptista, AEDM. Solution of advection-dominated transport by Eulerian-Lagrangian methods using the backwards method of characteristics. *Doctoral dissertation, Massachusetts Institute of Technology* 1987.

[4] Bravo R, Ortiz P, Idelsohn S, Becker P. Sediment transport problems by the particle finite element method (PFEM). *Computational Particle Mechanics* 2020; **7(1)**:139-149.

[5] Brooks AN, Hughes TJR. Streamline Upwind/Petrov–Galerkin formulations for the convective dominated flows with particular emphasis on the incompressible Navier-Stokes equations. *Computer Methods in Applied Mechanics and Engineering* 1982; **32** (1–3):199–259.

[6] Burridge HC, Parker DA, Kruger ES, Partridge JL, Linden PF. Conditional sampling of a high Péclet number turbulent plume and the implications for entrainment. *Journal of Fluid Mechanics* 2017 **823**:26-56.

[7] Cady R, Neuman SP. Three-dimensional adaptive Eulerian-Lagrangian finite element method for advection-dispersion. *Developments in Water Science* 1988; **36**:183-193.

[8] Cady, R. An adaptive multi-dimensional Eulerian-Lagrangian finite element method for simulating advection-dispersion. 1989.

[9] Chiumenti M, Valverde Q, De Saracibar CA, Cervera M. A stabilized formulation for incompressible elasticity using linear displacement and pressure interpolations. *Computer Methods in Applied Mechanics and Engineering* 2002; **191(46)**:5253–5264.

[10] Codina R. Comparison of some finite element methods for solving the diffusion-convection-reaction equation, *Computer Methods in Applied Mechanics and Engineering* 1998, 156:185-210.

[11] Codina R. On stabilized finite element methods for linear systems of convection–diffusion–reaction equations, *Computer Methods in Applied Mechanics and Engineering* 2000a, 190:2681-2706.

[12] Donea J. A Taylor-Galerkin method for convective transport problems, *International Journal for Numerical Methods in Engineering* 1984, 20:101-119.

[13] Douglas J, Russell TF. Numerical methods for convection-dominated diffusion problems based on combining the method of characteristics with the finite element or finite difference procedures, *SIAM Journal of Numerical Analysis* 1982, 19:871-885.

[14] Duan HY, Hsieh PW, Tan RC, Yang SY. Analysis of a new stabilized finite element method for the reaction–convection–diffusion equations with a large reaction coefficient. *Computer Methods in Applied Mechanics and Engineering* 2012; **247**: 15-36.

[15] Duan HY, Qiu F. A new stabilized finite element method for advection-diffusion-reaction equations. *Numerical Methods for Partial Differential Equations* 2016; **32(2)**: 616-645.

[16] Felippa C, Oñate E. Nodally exact Ritz discretizations of the 1D diffusion-absorption and Helmholtz equations by variational FIC and modified equation methods, *Computational Mechanics* 2007, 39(2):91-111.

[17] Franca LP, Dutra do Carmo EG. The Galerkin gradient least-squares method, *Computer Methods in Applied Mechanics and Engineering* 1989, 74:41-54.

[18] Franca LP, Valentin F. On an improved unusual stabilized finite element method for the advective-reactive-diffusive equation, *Computer Methods in Applied Mechanics and Engineering* 2001, 190:1785-1800.

[19] Gimenez JM, González LM. An extended validation of the last generation of particle finite element method for free surface flows. *Journal of Computational Physics* 2015; **284**:186-205.

[20] Gimenez J, Nigro N, Idelsohn S. Improvements to solve diffusion-dominant problems with PFEM-2. 2012.

[21] Harari I, Hughes TJR. Stabilized finite element methods for steady advection-diffusion with production, *Computer Methods in Applied Mechanics and Engineering* 1994; **115**:165-191.

[22] Healy RW, Russell TF. Solution of the advection-dispersion equation in two dimensions by a finite-volume Eulerian-Lagrangian localized adjoint method. *Advances in Water Resources* 1998; **21(1)**, 11-26.

[23] Hughes TJR, Brooks AN. A theoretical framework for Petrov–Galerkin methods, with discontinuous weighting functions: application to the streamline upwind procedure, in Gallagher RH, Norrie DM, Oden JT, Zienkiewicz OC (eds.), *Finite Elements in Fluids* 1982, IV,Wiley, Chichester.

[24] Hughes TJR, Mallet M. A new finite element formulations for computational fluid dynamics: III. The generalized streamline operator for multidimensional advective-diffusive systems. *Comput Methods Appl. Mech. Engrg.* 1986a, 58:305–328.

[25] Hughes TJR, Franca LP, Hulbert GM. A new finite element formulation for computational fluid dynamics: VIII. The Galerkin/least-squares method for advective-diffusive equations, *Computer Methods in Applied Mechanics and Engineering* 1989, 73:173-189.

[26] Hughes TJR, Feijoo GR, Mazzei L, Quincy JB. The variational multiscale method: a paradigm for computational mechanics, *Computer Methods in Applied Mechanics and Engineering* 1998, 166:3-24.

[27] Idelsohn S, Oñate E, Nigro N, Becker P, Gimenez J. Lagrangian versus Eulerian integration errors. *Computer Methods in Applied Mechanics and Engineering* 293 (2015) 191-206.

[28] Idelsohn SR, Marti J, Becker P, Oñate E. Analysis of multifluid flows with large time steps using the particle finite element method *International Journal for Numerical Methods in Engineering* 75 (2014) 621–644

[29] Idelsohn S, Nigro N, Gimenez J, Rossi R, Marti J. A fast and accurate method to solve the incompressible Navier-Stokes equations. *Engineering Computations: Int J for Computer-Aided Engineering* 30 (2013) 197-222

[30] S.R. Idelsohn, N.M. Nigro, A. Limache, E. Oñate. Large time-step explicit integration method for solving problems with dominant convection, *Comput. Methods Appl. Mech. Engrg.* 217–220 (2012) 168–185.

[31] Kikuchi F, Ushijima T. Theoretical analysis of some finite element schemes for convective diffusion equations, in: R. Gallagher, D. Norrie, J. Oden, O. C. Zienkiewicz (Eds.), Finite Elements in Fluids, Vol. IV, John Wiley and Sons Ltd, Chichester, 1982.

[32] Lazarov RD, Mishev ID, Vassilevski PS. Finite volume methods for convection-diffusion problems. *SIAM Journal on Numerical Analysis* 1996; **33(1)**:31-55.

[33] Löhner R, Morgan K, Zienkiewicz OC. The solution of non-linear hyperbolic equation systems by the finite element method, *International Journal for Numerical Methods in Fluids* 1984, 4:1043-1063.

[34] van de Meent JW, Tuval I, Goldstein RE. (2008). Nature's microfluidic transporter: rotational cytoplasmic streaming at high Péclet numbers. *Physical Review Letters* 2008 **101(17)**:178102.

[35] Nadukandi P, Oñate E, García Espinosa J. A high-resolution Petrov-Galerkin method for the 1D convection-diffusion-reaction problem, *Computer Methods in Applied Mechanics and Engineering* 2010, 199(9–12):525-546.

[36] Nadukandi P, Oñate E, García Espinosa J. A high-resolution Petrov-Galerkin method for the convection-diffusion-reaction problem. Part II. A multidimensional extension, *Computer Methods in Applied Mechanics and Engineering* 2012, 213-216:327-352.

[37] Nepf H. 1.061 / 1.61 Transport Processes in the Environment. *Massachusetts Institute of Technology: MIT OpenCourseWare* https://ocw.mit.edu/ License: Creative Commons BY-NC-SA.

[38] Neuman SP, Sorek S. Eulerian-Lagrangian methods for advection-dispersion. *Finite elements in water resources* 1982, 849-876

[39] Oñate E, Idelsohn SR, Zienkiewicz OC, TaylorRL, Sacco C. A stabilized finite point method for analysis of fluid mechanics problems. *Computer Methods in Applied Mechanics and Engineering* 1996, 139:315–346.

[40] Oñate E. Derivation of stabilized equations for numerical solution of advective-diffusive transport and fluid flow problems. *Computer Methods in Applied Mechanics and Engineering* 1998, 151:233-265.

[41] Oñate E. A stabilized finite element method for incompressible viscous flows using a finite increment calculus formulation. *Computer methods in applied mechanics and engineering* 2000; **182(3-4)**:355-370.

[42] Oñate E, Idelsohn SR. A mesh-free finite point method for advective-diffusive transport and fluid flow problems. *Comput. Mech.* 1998, 23:283–292.

[43] Oñate E, Manzan M. A general procedure for deriving stabilized space-time finite element methods for advective-diffusive problems. *Int. J. Num. Meth. Fluids* 1999, 31:203–221.

[44] Oñate E, Manzan M. Stabilization techniques for finite element analysis of convection-diffusion problems, in Sundén B, Comini G. (eds.), *Computational Analysis of Convection Heat Transfer* 2000, 71-117, WIT Press, Southampton (UK), 2000.

[45] Oñate E, Sacco C, Idelsohn SR. A finite point method for incompressible flow problems. *Computing and Visualization in Science* 2000, 2:67–75.

[46] Oñate E, García J. A finite element method for fluid-structure interaction with surface waves using a finite calculus formulation. *Computer Methods in Applied Mechanics and Engineering* 2001, 191:635–660.

[47] Oñate E, Perazzo F, Miquel J. A finite point method for elasticity problems. *Computers and Structures* 2001, 79:2151–2163.

[48] Oñate E, Taylor RL, Zienkiewicz OC, Rojek J. A residual correction method based on finite calculus. *Engineering Computations* 2003, 20(5/6):629–658.

[49] Oñate E, Idelsohn SR, Felippa C. Consistent pressure laplacian stabilization for incompressible continua via higher-order finite calculus. *International Journal for Numerical Methods in Engineering* 2011; **87(1-5)**:171–195.

[50] Oñate E, Franci A, Carbonell JM. Lagrangian formulation for finite element analysis

of quasi-incompressible fluids with reduced mass losses. *International Journal for Numerical Methods in Fluids* 2014; **74(10)**:699–731.

[51] Oñate E, Idelsohn SR, Del Pin F, Aubry R. The particle finite element method. An overview. *International Journal of Computational Methods* 2004, 1(2):267–307.

[52] Oñate E, Zarate F, Idelsohn SR. Finite element formulation for the convective-diffusive problems with sharp gradients using finite calculus, *Computer Methods in Applied Mechanics and Engineering* 2006, 195:1793-1825.

[53] Oñate E, Miquel J, Hauke G. Stabilized formulation for the advection-diffusion-absorption equation using finite calculus and linear finite elements, *Computer Methods in Applied Mechanics and Engineering* 2006, 195(33–36):3926–3946.

[54] Oñate E, Rojek J, Taylor RL, Zienkiewicz OC. Finite calculus formulation for incompressible solids using linear triangles and tetrahedra. *International Journal for Numerical Methods in Engineering* 2004; **59(11)**:1473–1500.

[55] Oñate E, Valls A, García J. FIC/FEM formulation with matrix stabilizing terms for incompressible flows at low and high Reynolds numbers. *Computational Mechanics* 2006, 38(4-5):440–455.

[56] Oñate E, García J, Idelsohn SR, Del Pin F. FIC formulations for finite element analysis of incompressible flows. Eulerian, ALE and Lagrangian approaches. *Computer Methods in Applied Mechanics and Engineering* 2006, 195(23-24):3001–3037.

[57] Oñate E, Miquel J, Zarate F. Stabilized solution of the multidimensional advection-diffusion-absorption equation using linear finite elements, *Computers and Fluids* 2007, 36:92–112.

[58] Oñate E, Valls A, García J. Modeling incompressible flows at low and high Reynolds numbers via a finite calculus-finite element approach. *Journal of Computational Physics* 2007, 224:332–351.

[59] Oñate E, Idelsohn SR, Celigueta MA, Rossi R. Advances in the particle finite element method for the analysis of fluid-multibody interaction and bed erosion in free surface flows. *Comput. Methods Appl. Mech. Engrg.* 2008, 197(19-20):1777—1800.

[60] Oñate E, Nadukandi P, Idelsohn S, García J, Felippa C. A family of residual-based stabilized finite element methods for Stokes flows. *Int. J. Num. Meth. in Fluids* 2011, 65 (1-3):106–134.

[61] Oñate E, Idelsohn SR, Felippa C. Consistent pressure Laplacian stabilization for incompressible continua via higher order finite calculus. *International Journal for Numerical Methods in Engineering* 2011, 87 (1-5):171—195.

[62] Oñate E, Nadukandi P, Idelsohn S. P1/P0+ elements for incompressible flows with discontinuous material properties. *Comput. Methods Appl. Mech. Engrg.* 2014, 271:185–209

[63] Oñate E, Miquel J, Nadukandi P. An accurate FIC-FEM formulation for the 1D advection–diffusion–reaction equation. *Comput. Methods Appl. Mech. Engrg.* 2016, 298:373–406.

[64] Oñate E, Nadukandi P, Miquel J. Accurate FIC-FEM formulation for the multidimensional steady-state advection–diffusion–absorption equation. *Comput. Methods Appl. Mech. Engrg.* 2017, 327:352-368.

[65] Puigferrat A, de-Pouplana I, Oñate E. FIC–FEM formulation for the multidimensional transient advection–diffusion–absorption equation. *Computer Methods in Applied Mechanics and Engineering* 2020; **365**:112984.

[66] Rossi LF. A comparative study of Lagrangian methods using axisymmetric and deforming blobs. SIAM Journal on Scientific Computing 2006; **27(4)**:1168-1180.

[67] Ruan F, McLaughlin D. An investigation of Eulerian-Lagrangian Methods for solving heterogeneous advection-dominated transport problems. *Water Resources Research* 1999; **35(8)**:2359-2373.

[68] Sevilla R, Fernández-Méndez S, Huerta A. Comparison of high-order curved finite elements, *International Journal for Numerical Methods in Engineering* 2011; **87(8)**:719-734.

[69] Thomson DJ. Eulerian analysis of concentration fluctuations in dispersing plumes and puffs. *Physics of Fluids* 1997; **9(8)**:2349-2354.

[70] Wang K, Wang H, Al-Lawatia M. An Eulerian-Lagrangian discontinuous Galerkin method for transient advection-diffusion equations. *Numerical Methods for Partial Differential Equations: An International Journal* 2007; **23(6)**:1343-1367.

[71] Wang K. A uniform optimal-order estimate for an Eulerian-Lagrangian discontinuous Galerkin method for transient advection–diffusion equations. *Numerical Methods for Partial Differential Equations: An International Journal* 2009; **25(1)**:87-109.

[72] Wang K, Wang H. A uniform estimate for the MMOC for two-dimensional advection-diffusion equations. *Numerical Methods for Partial Differential Equations: An International Journal* 2010; **26(5)**:1054-1069.

[73] Young DL, Wang YF, Eldho, TI. Solution of the advection–diffusion equation using the Eulerian–Lagrangian boundary element method. *Engineering analysis with boundary elements* 2000; **24(6)**:449-457.

[74] Young DL, Fan CM, Tsai CC, Chen CW, Murugesan K. Eulerian-Lagrangian method of fundamental solutions for multi-dimensional advection-diffusion equation *Doctoral dissertation, National Taiwan University* 2006

[75] Zienkiewicz OC, Codina R. A general algorithm for compressible and incompressible flows. Part I: the split, characteristic based scheme, *International Journal for Numerical Methods in Fluids* 1995, 20:869-885.

[76] Zienkiewicz OC, Taylor RL, Zhu JZ. *The finite element method. The basis.* 6th Ed., Elsevier, 2005.

[77] Zienkiewicz OC, Taylor RL, Nithiarasu P. *The finite element method for fluid dynamics.* 6th Ed., Elsevier, 2005.